

**Microwave photonic signal generation in an optically injected discrete mode semiconductor laser**

Chang, Da; Zhong, Zhuqiang; Valle, Angel; Jin, Wei; Jiang, Shan; Tang, Jianming; Hong, Yanhua

Photonics

DOI:
[10.3390/photonics9030171](https://doi.org/10.3390/photonics9030171)

Published: 10/03/2022

Peer reviewed version

[Cyswllt i'r cyhoeddiad / Link to publication](#)

Dyfyniad o'r fersiwn a gyhoeddwyd / Citation for published version (APA):
Chang, D., Zhong, Z., Valle, A., Jin, W., Jiang, S., Tang, J., & Hong, Y. (2022). Microwave photonic signal generation in an optically injected discrete mode semiconductor laser. *Photonics*, 9(3), Article 171. <https://doi.org/10.3390/photonics9030171>

Hawliau Cyffredinol / General rights

Copyright and moral rights for the publications made accessible in the public portal are retained by the authors and/or other copyright owners and it is a condition of accessing publications that users recognise and abide by the legal requirements associated with these rights.

- Users may download and print one copy of any publication from the public portal for the purpose of private study or research.
- You may not further distribute the material or use it for any profit-making activity or commercial gain
- You may freely distribute the URL identifying the publication in the public portal ?

Take down policy

If you believe that this document breaches copyright please contact us providing details, and we will remove access to the work immediately and investigate your claim.

Microwave photonic signal generation in an optically injected discrete mode semiconductor laser

Da Chang ¹, Zhuqiang Zhong ¹, Angel Valle ², Wei Jin ¹, Shan Jiang ¹, Jianming Tang ¹ and Yanhua Hong ^{1,*}

¹ School of Computer Science and Electronic Engineering, Bangor University, Bangor LL57 1UT, UK

² Instituto de Física de Cantabria (IFCA), Universidad de Cantabria-CSIC, Santander, Spain

* Correspondence: y.hong@bangor.ac.uk

Abstract: In this paper, microwave photonic signal generation based on period-one dynamic of optically injected discrete mode (DM) semiconductor lasers has been experimentally demonstrated and numerically simulated. The results show that the frequency of the generated microwave increases linearly with the frequency detuning or optical injection ratio. In addition, a single optical feedback loop is sufficient to reduce the microwave linewidth without significantly deteriorating side mode suppression. The simulation results using a model considering the nonlinear dependencies of the carrier recombination agree well with the experimental results, which indicates that the nonlinear carrier recombination effect is important in determining the nonlinear dynamics of optically injected DM lasers.

Keywords: Microwave photonics signal generation; discrete mode semiconductor laser; optical injection

1. Introduction

In the fast-developing information society, radio and microwave signals play significant roles in the field of communication, radar, and sensing systems [1-3]. To implement high speed transmission in wireless networks as well as high-resolution detection in radar and sensing systems, high-frequency microwave signals with salient features such as ultra-low phase noise and broad tunable range is highly required. However, it is complicated and costly to generate such desired high-frequency microwaves by multiple frequency doubling based on conventional electronic circuits [4]. Moreover, such high-frequency electrical microwave signals inevitably suffer enormous attenuation in coaxial cable transmissions for most practical scenarios [5]. To address these technical challenges, photonic approach, well-known as microwave photonics, has been applied to overcome the bottleneck of microwave generation in electrical domain. Generally speaking, photonic generation of microwave signals have superior advantages in terms of high frequency (up to millimeter-wave band), broad frequency tunability, low propagation loss in optical fibers and high robustness to electromagnetic interference [6-36]. Additionally, recently reported InP and silicon based photonic integrated devices/circuits [6-8] further expand the perspective of photonic high-frequency microwave and thus it becomes a very hot research topic in the field of radio-over-fiber (RoF), optical signal processing, true-time delay beamforming, and subnoise detection etc. [9-12].

Compared with the microwave synthesis using electronics, which has been extensively explored and developed over the past decades, high-frequency microwave photonic (MWP) signal generation in the optical domain is more convenient and cost-effective. Various approaches of MWP signal generation can generally be classified into optical heterodyning [13,14], direct and external modulation [15-17], self-pulsating and mode-locking [18,19], optoelectronic oscillators (OEOs) [20-24], and laser dynamics of period-one (P1) [25-36]. The optical heterodyne technique can easily achieve terahertz photonic

Citation: Lastname, F.; Lastname, F.; Lastname, F. Title. *Photonics* **2021**, *8*, x. <https://doi.org/10.3390/xxxxx>

Received: date

Accepted: date

Published: date

Publisher's Note: MDPI stays neutral with regard to jurisdictional claims in published maps and institutional affiliations.



Copyright: © 2021 by the authors. Submitted for possible open access publication under the terms and conditions of the Creative Commons Attribution (CC BY) license (<https://creativecommons.org/licenses/by/4.0/>).

microwaves by beating between two optical beams with certain wavelength spacing, as such the technique has very wide tunability [13]. However, the inevitable mismatch of optical phases and fluctuated amplitudes between two non-coherent lasers result in extremely poor microwave stability, which becomes an Achilles' heel for applications requiring high stability. Direct and external modulation schemes are also very important for high-frequency MWP signal generation. The former possesses the simplest architecture for MWP signal generation, but its modulation bandwidth is limited by the relaxation oscillation frequency of the lasers, which is usually less than 15GHz, and the modulation depth is also relatively low [15]. On the other hand, MWP signal generation utilizing external modulation can attain very high frequency and low phase noise microwave signals, but there is a drawback resulting from the insertion loss of the modulators [16]. An OEO is another paradigmatic method to obtain narrow-linewidth microwave signals in both the electrical and optical domains by introducing a feedback loop as a high-quality-factor optoelectronic oscillating cavity to a pump laser [20-24]. Consequently, the phase noise of generated microwaves can be comparable with those produced by mode-locked lasers [19], but the frequency tunability is compromised.

Recently, a competitive approach of MWP signal generation based on P1 dynamic of semiconductor lasers has been proposed and explored [25-36]. P1 dynamic of semiconductor lasers can be achieved by optical injection under certain injection parameters, which causes the optical output intensity of semiconductor lasers to undergo self-sustained oscillation at a microwave frequency [25]. The MWP signal is generated when the optical output of semiconductor lasers at P1 dynamic is detected by a photodetector. Due to the injection pulling effect and the red shifting effect, the generated photonic microwave frequency can be tens of times higher than the relaxation resonance frequency of the semiconductor laser while a relatively simple system setup still remains to support flexible tunability [26]. Therefore, considering the characteristics such as cost, power effectiveness and all-optical broad frequency tunability, MWP signal generation based on P1 dynamic of semiconductor lasers become a promising method, which has been widely studied for different types of semiconductor lasers. For distributed feedback (DFB) semiconductor lasers, Chan et al. comprehensively studied the P1 dynamic based photonic microwave generation, transmission, processing as well as its single sideband (SSB) characteristics [27-29]. Wang et al. reported continuous tunable photonic microwave generation in quantum dot semiconductor lasers [30]. For vertical-cavity surface-emitting lasers (VCSELs), Perez et al. achieved more than 20 GHz MWP signal using a single-mode VCSEL [31]. Lin et al. experimentally demonstrated microwave generation in multi-transverse-mode VCSELs by dual-beam orthogonal optical injection [32]. Li et al. numerically investigated the effect of birefringence-induced oscillation on the photonic microwave in spin-VCSELs [33]. We experimentally and theoretically studied broad tunable photonic microwave in optically injected VCSELs and discussed the suppression of second harmonic distortion [34-36]. Furthermore, to improve the quality of P1 dynamics based photonic microwave, extensive research efforts have also been made, which mainly include extra RF sources-enabled subharmonic locking and stabilization [37] and optical self-locking methods, such as optoelectronic feedback [38], single and double external cavity optical feedback [27].

As a special type of Fabry-Perot semiconductor lasers, discrete mode (DM) lasers have similar geometry structure with standard Fabry-Perot lasers but contain a small number of etching features along the ridge waveguide. This unique feature guarantees DM lasers achieving single longitudinal mode operation with high sidemode suppression [39]. DM lasers also have many other impressive characteristics, such as, very narrow linewidth, wide temperature operation range, low cost, and easy integration [40]. These salient features undoubtedly imply that DM lasers are a good candidate for P1 dynamic based low phase noise photonic microwave generation. However, the previous reports on DM lasers [41-42] do not address the photonic microwave generation in optically injected DM lasers. Therefore, in this paper, we focus on photonic microwave generation based on

period-one dynamic of optically injected DM semiconductor lasers. The main parameters affecting the fundamental frequency, power, linewidth, and phase noise of the generated photonic microwave have been experimentally studied. In addition, optical feedback is also adopted to further optimize the linewidth of the generated microwave. Finally, a modified rate equation model is proposed to numerically analyze the frequency of the generated microwave in DM lasers.

2. Experimental Setup

The schematic diagram of the experimental setup in a slave – master lasers configuration is illustrated in Figure 1. In this experiment, a commercially available TO-56 can-packaged fiber pigtailed DM laser (Eblana Photonics EP1550-DM-01-FA) with a lasing wavelength of about 1550 nm is used as a slave laser (SL). The DM laser is driven by an ultra-low noise current source (YOKOGAWA, GS200) and the temperature is stabilized at 24 °C by a temperature controller (Tektronix, TED 200) with an accuracy of 0.01 °C. A tunable laser (Agilent 8164A) is used as a master laser (ML). The emission of the ML injects into the SL after traveling through a polarization controller (PC1), a 50: 50 fiber coupler (FC1) and an optical circulator (OC). The PC1 is used to match the polarization of the injection beam to the SL’s polarization. The output of the DM laser passes through the OC and is divided into a feedback path and a detection path by a 90: 10 fiber coupler (FC2). The feedback loop composes of PC2, a variable attenuator (VA) and FC1. The polarization of the feedback light is controlled by PC2 to be parallel to the polarization of the DM laser. The detection path is further split by FC3 and the light beams are detected by a photodetector (PD, RXM40AF, 40 GHz bandwidth) and a high resolution optical spectrum analyzer (OSA, APEX 2070, 4 pm resolution), respectively. The output of the PD is recorded by an electrical spectrum analyzer (ESA, Anritsu MS2667C, 30 GHz bandwidth) or an oscilloscope (OSC, Tektronix 71254C, 12.5 GHz bandwidth).

The DM laser is biased at 30 mA, which is 2.5 times of its threshold current. Under this operation condition, the output power of the free-running DM laser is 0.6 mW, and the relaxation oscillation frequency is about 6.2 GHz. In this paper, the optical injection ratio (ξ_{inj}) is defined as the optical injection power divided by the output power of the free running DM laser, and the injection power is measured just before the injection beam enters the SL. The feedback ratio is defined as the ratio between the feedback power and the free running DM laser output power. The feedback power is measured just before the feedback beam is fed into the DM laser. The frequency detuning (Δf) is defined as $f_{inj} - f_{SL}$, where f_{inj} and f_{SL} are the frequencies of the ML and the free running SL, respectively. ξ_{inj} and Δf can be tuned by adjusting the output power and the frequency of the ML, respectively, and the feedback ratio is controlled by tuning the VA.

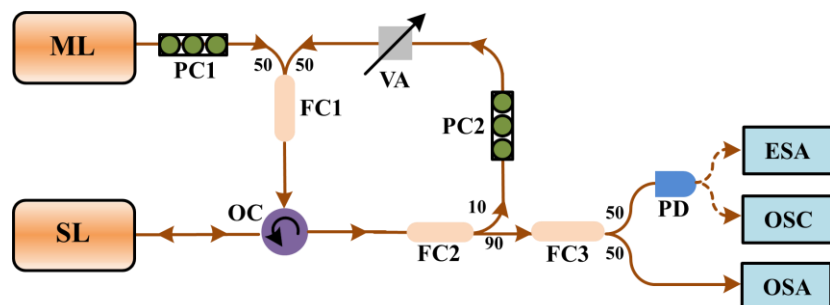


Figure 1. Schematic of the experimental setup. ML: master laser, SL: slave laser, PC: polarization control, FC: fiber coupler, OC: optical circulator, VA: variable attenuator, PD: photodetector, ESA: electrical spectrum analyzer, OSA: optical spectrum analyzer, OSC: oscilloscope.

3. Experimental Results

Firstly the dynamical evolution of the DM laser subject to optical injection is examined. The DM laser subject to optical injection without applying optical feedback is achieved by disconnecting PC2 from the rest experimental setup. Figure 2 displays the (a) time series, (b) power spectra, (c) optical spectra and (d) phase portraits of dynamical behaviours of the DM laser with different ξ_{inj} when Δf is fixed at 10 GHz. The phase portrait is defined as the local N -th intensity as a function of $(N-1)$ -th intensity. When $\xi_{inj} = 0.06$ (row 1), obviously, the DM laser experiences Hopf bifurcation and oscillates at P1 state with a fundamental frequency (f_0) of 10.1 GHz. The tunability and quality of microwave generated in the optically injected DM laser based on P1 dynamic will be discussed in the next section. When ξ_{inj} is increased to 0.36 (row 2), the DM laser shows period two (P2) oscillation. Further increase ξ_{inj} to 0.56 (row 3), the laser is in chaos dynamic. The above results indicate that the optically injected DM laser enters chaos through period doubling.

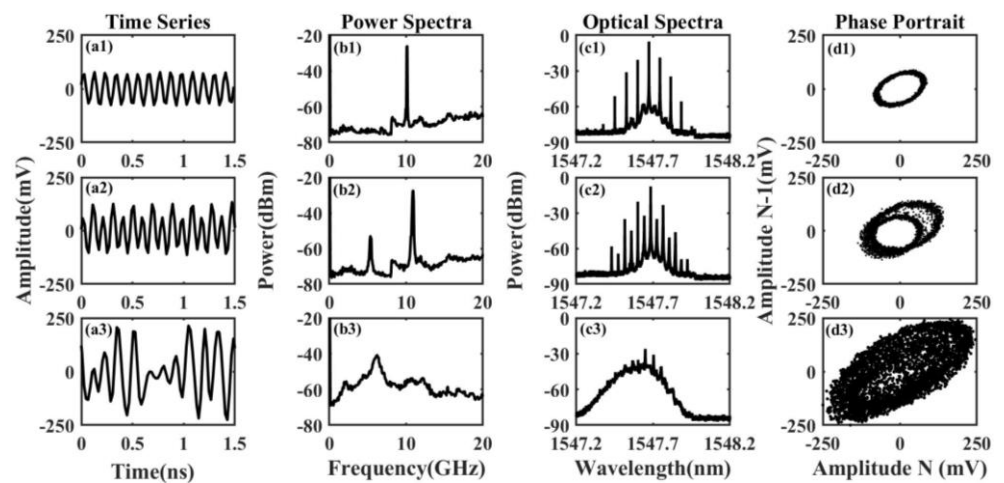


Figure 2. (a) Time series, (b) power spectra, (c) optical spectra and (d) phase portraits of the DM laser output when Δf is 10 GHz, and the injection ratio ξ_{inj} is 0.06 (row 1), 0.36 (row 2) and 0.56 (row 3).

In order to find P1 operation regions, the dynamics of the optically injected DM laser in a parameter space of frequency detuning Δf and injection ratio ξ_{inj} are measured and plotted in Figure 3. In the map, the stable (S), P1, P2, quasi period (QP) and chaos (C) dynamics are denoted by dark blue, light blue, green, orange, and red, respectively. Two non-P1 regions over the injection parameter space of $4\text{GHz} < \Delta f < 14\text{GHz}$ and $0.2 < \xi_{inj} < 1$, and $-16\text{GHz} < \Delta f < -8\text{GHz}$ and $0.1 < \xi_{inj} < 1$ are larger than those in DFB lasers [28], but P1 dynamic still dominates on the region above the Hopf bifurcation line.

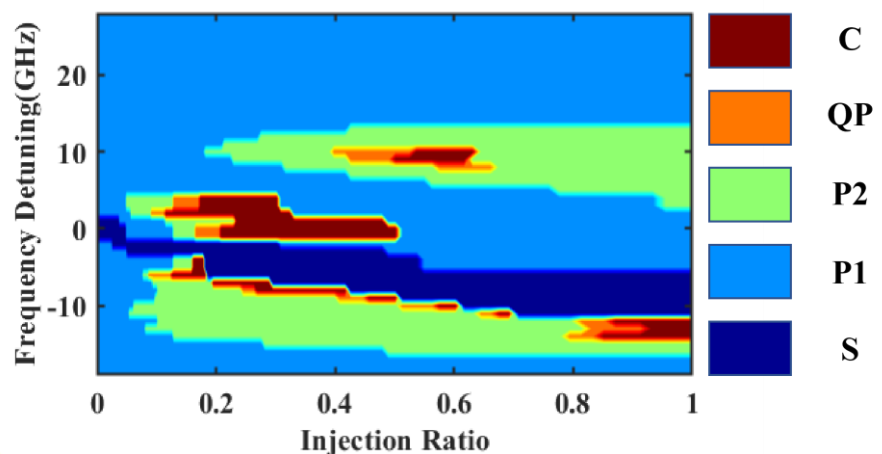


Figure 3. Dynamical map of the optically injected DM laser.

Now, we focus on MWP signal generation based on P1 dynamic in the optically injected DM laser. The effect of Δf and ξ_{inj} on the fundamental frequency (f_0) and the power of the generated microwave is presented in Figure 4. The power of the generated microwave is defined as the peak power at the fundamental frequency. Figure 4(a) shows the frequency of the generated microwave as a function of injection ratio. Three frequency detuning of 15GHz, 17GHz and 20GHz are studied here because the optically injected DM laser operates at P1 dynamic over a very wider injection ratio range with $\Delta f \geq 15$ GHz. The results reveal that the microwave frequency increases linearly with the increase of injection ratio, and the change rate of the microwave frequency drops when the frequency detuning increases, which is similar to that in the DFB laser and VCSEL [28, 34]. The relationship between the generated microwave power and the injection ratio is shown in Figure 4(b), which shows that the power of the generated microwave first increases as the injection ratio increases, when $\xi_{inj} = 0.92$, the microwave powers reach their maximum values. Further increasing the injection ratio, the microwave powers decrease again. The reason for the maximum power at the injection ratio of 0.92 is that the gain distribution of the semiconductor laser is affected by the optical injection, which causes the amplitudes of the red-shifted cavity resonance component and the regenerated injection component in the optical spectrum of P1 dynamic to change with the injection ratio. When the injection ratio is about 0.92, the amplitudes of the red-shifted cavity resonance component and the regenerative injection component are almost the same, therefore, the microwave power reaches its maximum [28, 48]. This phenomenon is similar to that in the DFB laser and VCSELs, where there is a maximum microwave power for a fixed frequency detuning [28, 34]. The impact of Δf on the frequency and power of the generated microwave photonic signal is investigated under two injection ratios: a lower injection ratio $\xi_{inj} = 0.1$, and a higher injection ratio $\xi_{inj} = 0.92$, as shown in Figure 4(c, d). There is no surprise that the microwave frequency increases with the increase of the frequency detuning because the main contribution of the generated microwave is the frequency beating of the red-shift cavity frequency and the regenerated injection frequency. The microwave power decreases with the increase of the frequency detuning due to the decrease of nonlinear frequency mixing effect with increasing Δf [29].

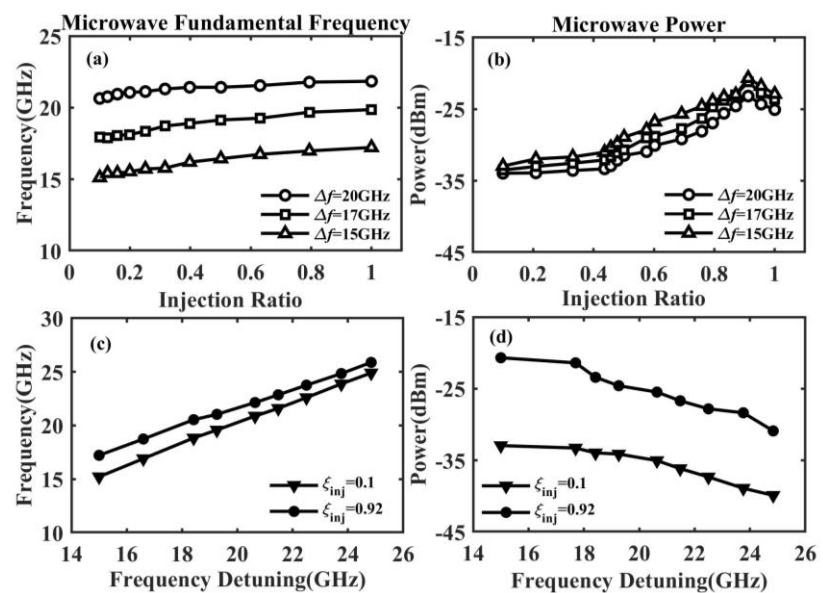


Figure 4. (a) Frequency and (b) power, of the generated microwave as function of injection ratio; (c) frequency and (d) power, of the microwave versus frequency detuning.

The quality of the generated microwave in the optically injected DM laser is examined by analyzing its linewidth and phase noise. A 3dB linewidth is adopted to quantify

the linewidth, and the phase noise is obtained by integrating single sideband power spectrum offset from 3 MHz to 200 MHz of the fundamental frequency and then normalized to the microwave power. The linewidth and phase noise of the generated microwave shown in Figure 4(a) are calculated and displayed in Figure 5. We can see that the linewidth and phase noise of the generated microwave decrease first with the increase of ξ_{inj} until they reach their minimum values at an injection ratio ξ_{inj} of around 0.92, further increasing the injection ratio, the linewidth and phase noise of the microwave signal increase again. The minimum linewidth and phase noise of the generated microwave obtained at the injection parameters $(\Delta f, \xi_{inj}) = (15 \text{ GHz}, 0.92)$ are 1.8 MHz and 2.75 rad², respectively. The microwave linewidths produced in the optically injected DM lasers are similar to those in DFB lasers [28], but narrower than those in VCSELs [35]. This is because DM lasers have very narrow linewidths [40]. Comparing Figure 5 with Figure 4(b), we can see that the linewidth and phase noise of the generated microwaves reach their local minima at the injection ratio where the maximum microwave power is achieved, these results are identical compared to those reported in DFB lasers [28].

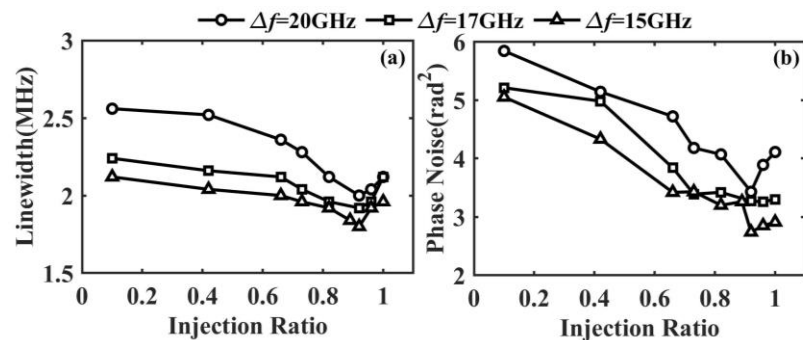


Figure 5. (a) Linewidth and (b) phase noise of the generated microwave versus ξ_{inj} .

In order to stabilize the fluctuation of the generated microwave and reduce its linewidth, the optical feedback technique used in DFB lasers and VCSELs [28, 43] is adopted. In this experiment, only a single feedback loop is introduced. Figure 6 presents the power spectra of the DM laser (a) without optical feedback and (b) with optical feedback at the injection parameters of $(\Delta f, \xi_{inj}) = (15 \text{ GHz}, 0.92)$. At these injection parameters, the fundamental frequency of the microwave is 17.2 GHz. As shown in Figure 6 (a), the linewidth of the generated microwave photonic signal is 1.8MHz without optical feedback. After introducing the optical feedback, the linewidth reduces. Figure 6(b) shows that the linewidth narrows from 1.82 MHz to 0.52 MHz when the feedback ratio is -27.8dB and the feedback round trip time is 96.15ns. Many side peaks equally separated by multiple of 10.4 MHz also appear in Figure 6(b), which corresponds to the external cavity modes' frequencies. To quantify the side peaks in the power spectrum, a concept of side peak suppression (SPS) is introduced and is defined as the ratio of the power at the fundamental frequency to the maximum power of the side peaks [43]. The SPS is around 28 dB as shown in Figure 6 (b).

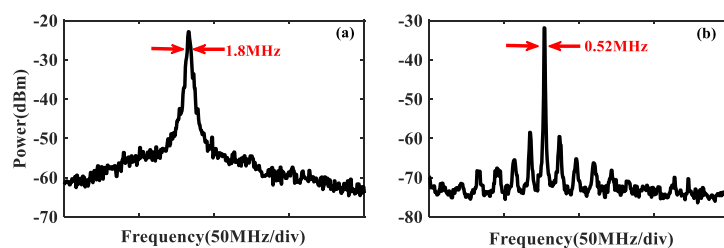


Figure 6. Power spectra of the DM laser (a) without, (b) with, optical feedback. The injection parameters $(\Delta f, \xi_{inj}) = (15 \text{ GHz}, 0.92)$.

The effect of the optical feedback ratio on the linewidth, phase noise and SPS of the generated microwave in the optically injected DM laser is studied and shown in Figure 7. The parameters in Figure 7 are the same as those in Figure 6(b) except for the optical feedback ratio. Figure 7(a) shows that the linewidth first decreases as the feedback ratio increases. When the feedback ratio is increased to -35.7dB, the linewidth remains almost constant as the feedback ratio is further increased until the feedback ratio reaches -25.7dB. Further increasing the optical feedback ratio, the linewidth increases again. This variation trend is different from that in the DFB laser and VCSEL [28, 35], but is similar to that in the DFB laser with filter feedback at some frequency detuning [44]. The relationship between the phase noise and the feedback ratio is similar to that of the linewidth. As the feedback ratio increases, the phase noise first decreases, then remains constant at around 0.3 rad², and then increases again. Figure 7 (c) presents SPS as a function of feedback ratio. When the feedback ratio is -42.7dB, the SPS is 30.3 dB. The SPS starts to decrease first when the feedback strength increases, which is similar to that in the DFB laser and VCSEL [28, 35]. But after the feedback ratio increases to -35.8 dB, further increasing the feedback ratio, the SPS remains almost constant at a value of about 28.3dB until the feedback ratio reaches -25.7dB. Beyond the aforementioned feedback ratio, the SPS decreases sharply. This is because the DM laser is about to leave P1 dynamic. Figure 7 shows that the SPS remains above 25dB within the feedback ratios where the linewidth and phase noise are kept to their minimum. The results indicate that a high SPS can be maintained over a wide feedback ratio range in the optically injected DM laser with a single optical feedback loop. The different variations shown in Figure 7 compared to those in DFB lasers and VCSELs may attribute to the filtering effect caused by the structure of the DM laser, but further study is needed to fully understand the characteristics of DM lasers.

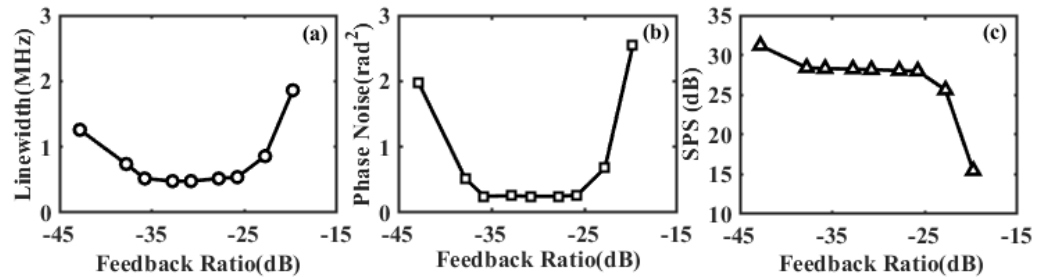


Figure 7. (a) Linewidth, (b) phase noise variance, (c) side peak suppression, of the generated microwave as a function of the feedback ratio. The injection parameters ($\Delta f, \xi_{inj}$) are (15 GHz, 0.92).

4. Theoretical model and analysis

Dynamics of the optically injected DM laser and the characteristics of the generated microwave based on P1 dynamic in the optically injected DM laser are numerically simulated using the model in [45] and by considering the nonlinear carrier recombination [46].

$$\frac{dE(t)}{dt} = \frac{(1+i\alpha)}{2} \left[\frac{g(N-N_0)}{1+\varepsilon|E(t)|^2} - \frac{1}{\tau_p} \right] E(t) + \eta E_{inj} e^{i2\pi\Delta f t} + \kappa E(t-\tau_{ext}) e^{-i\omega\tau_{ext}} \quad (1)$$

$$\frac{dN(t)}{dt} = \frac{I}{e} - (AN + BN^2 + CN^3) - \frac{g(N-N_0)|E(t)|^2}{1+\varepsilon|E(t)|^2} \quad (2)$$

where $E(t)$ is the slowly varying complex amplitude of the electric field, E_{inj} is the injection field amplitude. $N(t)$ represents the carrier number, α is the linewidth-enhanced factor, g is the differential gain coefficient, N_0 is the transparency carrier number and ε is the gain saturation factor, τ_p is the photon lifetime, τ_{ext} is the feedback round trip time of optical feedback loop, ω is the angular frequency of the laser, η denotes the injection

strength, κ denotes feedback strength from optical feedback loop, I is the injection current, e is the electron charge, A is the non-radiative modulus, B is the spontaneous modulus, C is the Auger recombination modulus. The parameter values used in [46] are adopted, where $\alpha = 3$, $g = 1.48 \times 10^4 \text{ s}^{-1}$, $I = 30 \text{ mA}$, $N_0 = 1.93 \times 10^7$, $\varepsilon = 7.73 \times 10^{-8}$, $\tau_p = 2.17 \text{ ps}$, $A = 2.8 \times 10^8 \text{ s}^{-1}$, $B = 9.8 \text{ s}^{-1}$, and $C = 3.84 \times 10^{-7} \text{ s}^{-1}$. The relaxation oscillation frequency of the free-running laser is approximate $f_r = (gE^2/\tau_p)^{1/2}/2\pi = 6.2 \text{ GHz}$. Eqs. (1), (2) are solved using the second-order Runge-Kutta algorithm.

The dynamical map of the DM laser in the parameter space of frequency detuning Δf and injection strength η is presented in Figure 8(a). The result qualitatively consistent with the experimental measurements in Figure 3. To validate the model used in the simulation, we also simulated the dynamical map of the DFB laser using the model and parameters of [47] and the results are shown in Figure 8(b). Figure 8(b) shows only one small non-P1 island within the P1 region above the Hopf bifurcation line, which is different from the experimental observation. Therefore, the nonlinear carrier recombination is necessary to be included for the investigation of the nonlinear dynamics of the optically injected DM laser.

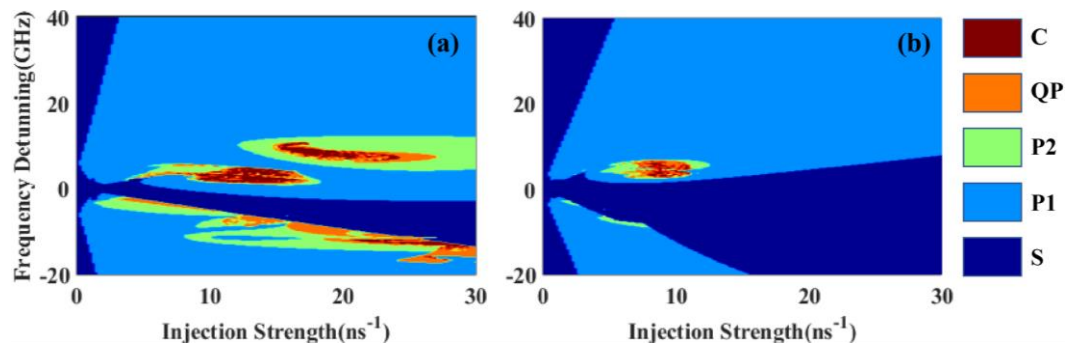


Figure 8. Numerical simulation of the dynamical maps of (a) the optically injected DM laser with the consideration of the nonlinear carrier recombination, (b) the optically injected DFB laser.

The SPS as a function of feedback strength for the generated MWP signal in the optically injected DM laser and DFB laser with single optical feedback is calculated and displayed in Figure 9. The injection parameters (Δf , η) are set at (15 GHz, 8 ns^{-1}), and the feedback round trip time is 10ns. Figure 9 shows that for the DM laser, the SPS is $\sim 17.1 \text{ dB}$ at the feedback strength of 0.32 ns^{-1} . When the feedback strength is increased, the SPS starts to drop, and when the feedback strength reaches 0.4 ns^{-1} , the SPS decreases to $\sim 14.1 \text{ dB}$. But further increasing the feedback strength, the SPS remains almost unchanged until the feedback strength reaches 0.5 ns^{-1} . Increase the feedback strength further, the SPS starts to deteriorate again. However, for the DFB laser, the SPS decreases monotonically with the increase of the feedback strength. These results are qualitatively consistent with our experimental results in the DM laser and the reported results in the DFB laser, which indicates that single optical feedback is sufficient to achieve a narrow microwave linewidth in the optically injected DM laser.

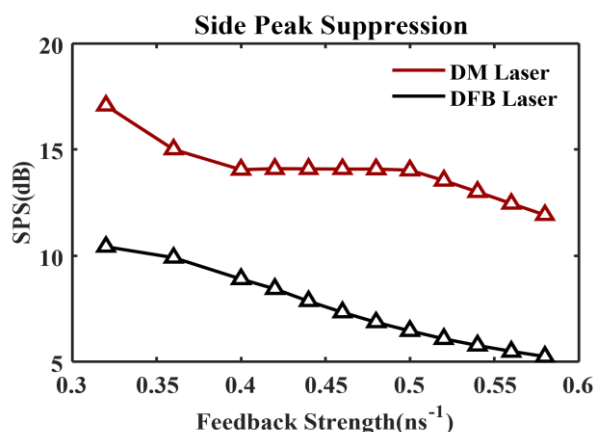


Figure 9. Numerical simulation of SPS of the generated microwave as a function of the feedback strength utilizing DM laser model and DFB laser model with the injection parameters $(\Delta f, \eta) = (15 \text{ GHz}, 8 \text{ ns}^{-1})$.

The variations of the fundamental frequency as a function of injection strength under two frequency detunings of 15 GHz and 20 GHz are calculated for the optically injected DM laser and optically injected DFB laser. The different variation of the fundamental frequency between the DM laser and DFB laser is illustrated in Figure 10. We can see that for the DFB laser, the fundamental frequency variation with the injection strength is similar to the report [48], where the frequency change rate for the lower injection strength is smaller compared to that for a higher injection strength. But for the optically injected DM laser, the fundamental frequency increases linearly with the injection strength. This linear relationship implies that DM lasers may be a better candidate for frequency-modulation continuous-wave microwave generation based on P1 dynamic.

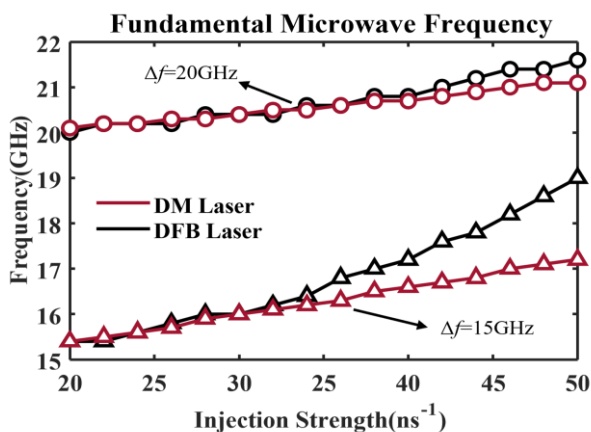


Figure 10. Numerical simulation of the generated microwave frequency as a function of the injection strength utilizing DM laser model and DFB laser model. $\Delta f = 15 \text{ GHz}$ and 20 GHz .

5. Discussion

In the experiment, due to the limitation of the bandwidth of the spectrum analyzer and the maximum output power of the ML, only the injection parameters with the injection ratio ≤ 1 and the frequency detuning $\leq 26 \text{ GHz}$ are investigated. The experimental results show that the fundamental microwave frequency increases linearly with the increase of the frequency detuning and injection ratio. It has been reported that the generated microwave frequency at strong injection ratio still increases linearly with the injection ratio in other types of lasers [34, 48]. The properties of the MWP signal generation in the DM laser

at larger frequency detuning and stronger injection power will be investigated in future studies. The linewidth of the generated microwave is related to the linewidth of the ML and SL, therefore, the generated microwave linewidth in the DM laser is comparable to that in the DFB laser, and narrower than that in the VCSEL. In the experiment, the microwave linewidths produced in the optically injected DM lasers with and without optical feedback are still in the range of hundreds of kilohertz to several megahertz. The linewidth of the generated microwave in the DFB laser can be reduced to a few hertz or even millihertz by optical modulation sideband injection locking or opto-electronic feedback [49, 50]. Therefore, further reduction of the generated microwave linewidth in the DM laser will be undertaken in our next investigation. In addition, the relationship between the linewidth of the generated microwave and the feedback strength in an optically injected semiconductor laser subject to filtered optical feedback is related to the injection parameters [44], so it is worth further study the relationship between the linewidth and the feedback strength in the DM laser at other injection parameters.

6. Conclusions

In summary, we experimentally and theoretically investigate MWP signal generation based on P1 dynamic of an optically injected DM semiconductor lasers. The experimental results show that the frequency of the generated microwave can be tuned by changing optical injection ratio or frequency detuning. The results also show that the linewidth of the generated microwave in the DM laser is comparable to that in DFB lasers and narrower compared to that in VCSELs, which may be due to the narrow linewidth of the DM laser. In addition, by introducing optical feedback, the relationship between the linewidth and the feedback ratio in the DM laser is similar to that in the DFB laser with filter feedback, which can attribute to the filtering effect caused by the structure of the DM laser. Furthermore, a SPS of > 25 dB can remain over a wide range of the feedback ratio, this suggests that single optical feedback is sufficient for reducing the linewidth of the generated microwave in the DM laser. Numerical simulations with the consideration of the nonlinear carrier recombination confirms that high SPSs can be maintained over a wide range of optical feedback strength, which is in good agreement with the results obtained in the experiment.

Author Contributions: Conceptualization, Da Chang, Zhuqiang Zhong, Angel Valle, Yanhua Hong; Data curation, Da Chang, Zhuqiang Zhong, Yanhua Hong; Formal analysis, Da Chang, Zhuqiang Zhong, Yanhua Hong, Wei Jin, Shan Jiang; Funding acquisition, Yanhua Hong, Jianming Tang, Angel Valle; Investigation, Da Chang, Zhuqiang Zhong, Angel Valle, Yanhua Hong; Methodology, Da Chang, Zhuqiang Zhong, Jianming Tang, Yanhua Hong; Project administration, Yanhua Hong, Jianming Tang, Angel Valle; Software, Da Chang, Zhuqiang Zhong; Supervision, Zhuqiang Zhong, Yanhua Hong; Validation, Da Chang, Zhuqiang Zhong, Yanhua Hong; Visualization, Da Chang, Zhuqiang Zhong, Yanhua Hong; Writing – original draft, Da Chang, Zhuqiang Zhong; Writing – review & editing, Da Chang, Zhuqiang Zhong, Angel Valle, Wei Jin, Shan Jiang, Jianming Tang and Yanhua Hong.

Funding: This research was funded in part by the DESTINI project funded by the ERDF under the SMARTExpertise scheme, in part by the DSP Centre funded by the ERDF through the Welsh Government and in part by Ministerio de Ciencia e Innovación, Spain under grant RTI2018-094118-B-C22 MCIN/AEI/FEDER, UE.

Data Availability Statement: Not applicable

Acknowledgments: D. Chang thanks the support of Bangor University's Great Heritage PhD studentship.

Conflicts of Interest: The authors declare no conflict of interest.

References

1. Yao, J. Microwave Photonics. *J. Light. Technol.* **2009**, *27*, 314-335. 384
2. Pan, S.; Zhang, Y. Microwave photonic radars. *J. Light. Technol.* **2020** *38*, 5450-5484. 385
3. Nie, B.; Ruan, Y.; Yu, Y.; Guo, Q.; Xi, J.; Tong, J. Period-one microwave photonic sensing by a laser diode with optical feedback. *J. Light. Technol.* **2020**, *38*, 5423-5429. 386
4. William, J.; Shain, N. A.; Vickers, A. N.; Thomas, B.; Anne, S.; Jerome, M. Dual fluorescence-absorption deconvolution applied to extended-depth-of-field microscopy. *Opt. Lett.* **2017**, *42*, 4183-4186. 387
5. Xu, C.; Zhou, L.; Zhou, J.Y.; Boggs, S. High frequency properties of shielded power cable - part 1: overview of mechanisms. *IEEE Electrical Insulation Magazine* **2005**, *21*, 24-28. 388
6. Carpintero, G.; Balakier, K.; Yang, Z.; Guzmán, R. C.; Corradi, A.; Jimenez, A.; Kervella, G.; Fice, M. J.; Lamponi, M.; Chitoui, M.; van Dijk, F.; Renaud, C. C.; Wonfor, A.; Bente, E. A. J. M.; Penty, R. V.; White, I. H.; Seeds, A. J. Microwave Photonic integrated circuits for millimeter-wave wireless communications. *J. Light. Technol.* **2014**, *32*, 3495-3501. 389
7. Wu, J.; Peng, J.; Liu, B.; Pan, T.; Zhou, H.; Mao, J.; Yang, Y.; Qiu, C.; Su, Y. Passive silicon photonic devices for microwave photonic signal processing. *Opt. Communications* **2016**, *373*, 44-52. 390
8. Liu, J.; Lucas, E.; Raja, A. S.; He, J.; Riemensberger, J.; Wang, R. N.; Karpov, M.; Guo, H.; Bouchand, R.; Kippenberg, T. J. Photonic microwave generation in the X- and K-band using integrated soliton microcombs. *Nat. Photonics* **2020**, *14*, 486-491. 391
9. Islam, M. S.; Kovalev, A.V.; Coget, G.; Viktorov, E.A.; Citrin, D.S.; Locquet, A. Staircase dynamics of a photonic microwave oscillator based on a laser diode with delayed optoelectronic feedback. *Phys. Rev. Applied* **2020**, *13*, 064038. 392
10. Xie, X.; Bouchand, R.; Nicolodi, D.; Giunta, M.; Hänsel, W.; Lezius, M.; Joshi, A.; Datta, S.; Alexandre, C.; Lours, M.; Tremblin, P.A. Photonic microwave signals with zeptosecond-level absolute timing noise. *Nat. Photonics* **2017**, *11*, 44-47. 393
11. Xue, X.; Xuan, Y.; Bao, C.; Li, S.; Zheng, X.; Zhou, B.; Qi, M.; Weiner, A. M. Microcomb-based true-time-delay network for microwave beamforming with arbitrary beam pattern control. *J. Light. Technol.* **2018**, *36*, 2312-2321. 394
12. Bünermann, O.; Jiang, H.; Dorenkamp, Y.; Kandratsenka, A.; Janke, S.M.; Auerbach, D.J.; Wodtke, A.M. Electron-hole pair excitation determines the mechanism of hydrogen atom adsorption. *Science* **2015**, *350*, 1346-1349. 395
13. Gliese, U.; Nielsen, T.N.; Bruun, M.; Christensen, E.L.; Stubkjaer, K.E.; Lindgren, S.; Broberg, B. A wideband heterodyne optical phase-locked loop for generation of 3-18 GHz microwave carriers. *IEEE Photonics Technol. Lett.* **1992**, *4*, 936-938. 396
14. Kittlaus, E.A.; Eliyahu, D.; Ganji, S.; Williams, S.; Matsko, A.B.; Cooper, K.B.; Forouhar, S. A low-noise photonic heterodyne synthesizer and its application to millimeter-wave radar. *Nat. Communications* **2021**, *12*, 4397. 397
15. Hwang, S. K.; Chan, S. C.; Hsieh, S. C.; Li, C. Y. Photonic microwave generation and transmission using direct modulation of stably injection-locked semiconductor lasers. *Optics Communications*, **2011**, *284*, 3581-3589. 398
16. Gao, Y.; Wen, A.; Zheng, H.; Liang, D.; Lin, L. Photonic microwave waveform generation based on phase modulation and tunable dispersion. *Opt. Express* **2016**, *24*, 12524-12533. 399
17. He, Y.; Jiang, Y.; Zi, Y.; Bai, G.; Tian, J.; Xia, Y.; Zhang, X.; Dong, R.; Luo, H. Photonic microwave waveforms generation based on two cascaded single-drive Mach-Zehnder modulators. *Opt. Express* **2018**, *26*, 7829-7841. 400
18. Dal Bosco, A. K.; Kanno, K.; Uchida, A.; Sciamanna, M.; Harayama, T.; Yoshimura, K. Cycles of self-pulsations in a photonic integrated circuit. *Phys. Rev. E* **2015**, *92*, 062905. 401
19. Sooudi, E.; Huyet, G.; McInerney, J. G.; Lelarge, F.; Merghem, K.; Martinez, A.; Ramdane, A.; Hegarty, S. P. Observation of harmonic-mode-locking in a mode-locked InAs/InP-based quantum-dash laser with cw optical injection. *IEEE Photonics Technol. Lett.*, **2011**, *23*, 549-551. 402
20. Zou, X.; Liu, X.; Li, W.; Li, P.; Pan, W.; Yan, L.; Shao, L. Optoelectronic oscillators (OEOs) to sensing, measurement, and detection. *IEEE J. Quantum Electron.* **2015**, *52*, 1-16. 403
21. Liao, M. L.; Huang, Y. Z.; Weng, H. Z.; Han, J. Y.; Xiao, Z. X.; Xiao, J. L.; Yang, Y. D. Narrow-linewidth microwave generation by an optoelectronic oscillator with a directly modulated microsquare laser. *Opt. Lett.* **2017**, *42*, 4251-4254. 404
22. Lin, X. D.; Wu, Z. M.; Deng, T.; Tang, X.; Fan, L.; Gao, Z. Y.; Xia, G. Q. Generation of widely tunable narrow-linewidth photonic microwave signals based on an optoelectronic oscillator using an optically injected semiconductor laser as the active tunable microwave photonic filter. *IEEE Photon. J.* **2018**, *10*, 1-9. 405
23. Zhang, W.; Yao, J. Silicon photonic integrated optoelectronic oscillator for frequency-tunable microwave generation. *J. Light. Technol.* **2018**, *36*, 4655-4663. 406
24. Li, M.; Hao, T.; Li, W.; Dai, Y. Tutorial on optoelectronic oscillators. *APL Photonics* **2021**, *6*, 061101. 407
25. AlMulla, M.; Liu, J. M. Linewidth characteristics of period-one dynamics induced by optically injected semiconductor lasers. *Opt. Express* **2020**, *28*, 14677-14693. 408
26. Qi, X.; Liu, J. M. Photonic microwave applications of the dynamics of semiconductor lasers. *IEEE J. Sel. Topics. Quantum Electron* **2011**, *17*, 1198-1211. 409
27. Zhuang, J. P.; Chan, S. C. Tunable photonic microwave generation using optically injected semiconductor laser dynamics with optical feedback stabilization. *Opt. Lett.* **2013**, *38*, 344-346. 410
28. Zhuang, J. P.; Chan, S.C. Phase noise characteristics of microwave signals generated by semiconductor laser dynamics. *Opt. Express*. **2015**, *33*, 2777-2797. 411
29. Zhang, L.; Chan, S. C. Cascaded injection of semiconductor lasers in period-one oscillations for millimeter-wave generation. *Opt. Lett.* **2019**, *44*, 4905-4908. 412

30. Wang, C.; Raghunathan, R.; Schires, K.; Chan, S. C.; Lester, L. F.; Grillot, F. Optically injected InAs/GaAs quantum dot laser for tunable photonic microwave generation. *Opt. Lett.* **2016**, *41*, 1153-1156. 443-444
31. Perez, P.; Quirce, A.; Valle, A.; Consoli, A.; Noriega, I.; Pesquera, L.; Esquivias, I. Photonic generation of microwave signals using a single-mode VCSEL subject to dual-beam orthogonal optical injection. *IEEE Photonics J.* **2015**, *7*, 1-14. 445-446
32. Lin, H.; Ourari, S.; Huang, T.; Jha, A.; Briggs, A.; Bigagli, N. Photonic microwave generation in multimode VCSELs subject to orthogonal optical injection. *J. Opt. Soc. Am. B* **2017**, *34*, 2381-2389. 447-448
33. Huang, Y.; Zhou, P.; Li, N. Broad tunable photonic microwave generation in an optically pumped spin-VCSEL with optical feedback stabilization. *Opt. Lett.* **2021**, *46*, 3147-3150. 449-450
34. Ji, S.; Hong, Y.; Spencer, P.S.; Benedikt, J.; Davies, I. Broad tunable photonic microwave generation based on period-one dynamics of optical injection vertical-cavity surface-emitting lasers. *Opt. Express* **2017**, *25*, 19863-19871. 451-452
35. Ji, S.; Xue, C. P.; Valle, A.; Spencer, P. S.; Li, H. Q.; Hong, Y. Stabilization of photonic microwave generation in vertical-cavity surface-emitting lasers with optical injection and feedback. *J. Light. Technol.* **2018**, *32*, 4660-4666. 453-454
36. Valle, A.; Quirce, A.; Ji, S.; Hong, Y. Polarization effects on photonic microwave generation in VCSELs under optical injection. *Photon. Technol. Lett.* **2018**, *30*, 1266-1269. 455-456
37. Fan, L.; Wu, Z. M.; Deng, T.; Wu, J. G.; Tang, X.; Chen, J. J.; Mao, S.; Xia, G. Q. Subharmonic microwave modulation stabilization of tunable photonic microwave generated by period-one nonlinear dynamics of an optically injected semiconductor laser. *J. Light. Technol.* **2014**, *32*, 4660-4666. 457-459
38. Ma, X. W.; Huang, Y. Z.; Zou, L. X.; Liu, B. W.; Long, H.; Weng, H. Z.; Yang, Y. D.; Xiao, J. L. Narrow-linewidth microwave generation using AlGaInAs/InP microdisk lasers subject to optical injection and optoelectronic feedback. *Opt. Express* **2015**, *23*, 20321-20331. 460-462
39. Osborne, S.; O'Brien, S.; Buckley, K.; Fehse, R.; Amann, A.; Patchell, J.; Kelly, B.; Jones, D.R.; O'Gorman, J.; O'Reilly, E.P. Design of single-mode and two-color Fabry-Pérot lasers with patterned refractive index. *IEEE J. Sel. Top. Quantum Electron.* **2007**, *13*, 1157-1163. 463-465
40. Herbert, C.; Jones, D.; Kaszubowska-Anandarajah, A.; Kelly, B.; Rensing, M.; O'Carroll, J.; Phelan, R.; Anandarajah, P.; Perry, P.; Barry, L. P.; O'Gorman, J. Discrete mode lasers for communication applications. *IET Optoelectron.* **2009**, *3*, 1-17. 466-467
41. Rosado, A.; Pérez-Serrano, A.; Tijero, J.M.G.; Gutierrez, A.V.; Pesquera, L.; Esquivias, I. Numerical and experimental analysis of optical frequency comb generation in gain-switched semiconductor lasers. *IEEE J. Quantum Electron.* **2019**, *55*, 1-12. 468-469
42. Zhong, Z.; Chang, D.; Jin, W.; Lee, M. W.; Wang, A.; Jiang, S.; He, J.; Tang, J.; Hong, Y. Intermittent dynamical state switching in discrete-mode semiconductor lasers subject to optical feedback. *Photon. Res.* **2021**, *9*, 1336-1342. 470-471
43. Xue, C.; Chang, D.; Fan, Y.; Ji, S.; Zhang, Z.; Lin, H.; Spencer, P. S.; Hong, Y. Characteristics of microwave photonic signal generation using vertical-cavity surface-emitting lasers with optical injection and feedback. *J. Opt. Soc. Am. B* **2020**, *37*, 1394-1400. 472-473
44. Xue, C.; Ji, S.; Hong, Y.; Jiang, N.; Li, H.; Qiu, K. Numerical investigation of photonic microwave generation in an optically injected semiconductor laser subject to filtered optical feedback. *Opt. Express* **2018**, *27*, 5065-5082. 474-475
45. Dellunde, J.; Torrent, M. C.; Sancho, J. M.; San M. M. Frequency dynamics of gain-switched injection-locked semiconductor lasers. *IEEE J. Quantum Electron.* **1997**, *33*, 1537-1542. 476-477
46. Valle, A. Statistics of the optical phase of a gain-switched semiconductor laser for fast quantum randomness generation. *Photonics* **2021**, *8*, 388. 478-479
47. Li, N.; Pan, W.; Locquet, A.; Chizhevsky, V.N.; Citrin, D.S. Statistical properties of an external-cavity semiconductor laser: Experiment and theory. *IEEE J. Sel. Top. Quantum Electron.* **2015**, *21*, 553-560. 480-481
48. Chan, S. C.; Hwang S. K.; Liu, J. M. Period-one oscillation for photonic microwave transmission using an optically injected semiconductor laser. *Opt. Express* **2007**, *15*, 14921-14935. 482-483
49. Hung, Y.-H.; Hwang, S.-K. Photonic microwave stabilization for period-one nonlinear dynamics of semiconductor lasers using optical modulation sideband injection locking. *Opt. Express* **2015**, *23*, 6520-6532. 484-485
50. Suelzer, J. S.; Simpson, T. B.; Devgan, P.; Usechak, N. G. Tunable, low-phase-noise microwave signals from an optically injected semiconductor laser with opto-electronic feedback. *Opt. Lett.* **2017**, *42*, 3181-3184. 486-487